CHAPTER TEN

Rational Design of Nanoparticle Platforms for "Cutting-the-Fat": Covalent Immobilization of Lipase, Glycerol Kinase, and Glycerol-3-Phosphate Oxidase on Metal Nanoparticles

V. Aggarwal, C.S. Pundir[1]
Department of Biochemistry, Maharshi Dayanand University, Rohtak, Haryana, India
[1]Corresponding author: e-mail address: pundircs@rediffmail.com

Contents

1. Introduction 198
2. Use of Rationally Designed Nanoscaffolds for Enzyme Binding 200
3. Use of Chitosan for Enhancing Nanoparticle Surface Chemistry 201
4. Experimental 202
   4.1 Combined Assay of Mixture of Free/Native Lipase, GK and GPO 202
   4.2 Combined Assay of Enzymes 202
   4.3 Kinetic Properties of Co-Immobilized Lipase, GK, and GPO 215
   4.4 Application of Co-Immobilized Lipase, GK, and GPO onto Nanomaterials 219
References 222

Abstract

The aggregates of nanoparticles (NPs) are considered better supports for the immobilization of enzymes, as these promote enzyme kinetics, due to their unusual but favorable properties such as larger surface area to volume ratio, high catalytic efficiency of certain immobilized enzymes, non-toxicity of some of the nanoparticle matrices, high stability, strong adsorption of the enzyme of interest by a number of different approaches, and faster electron transportability. Co-immobilization of multiple enzymes required for a multistep reaction cascade on a single support is more efficient than separately immobilizing the corresponding enzymes and mixing them physically, since products of one enzyme could serve as reactants for another. These products can diffuse much more easily between enzymes on the same particle than diffusion from one particle to the next, in the reaction medium. Thus, co-immobilization of enzymes onto NP aggregates is expected to produce faster kinetics than their individual immobilizations on separate matrices. Lipase, glycerol kinase, and glycerol-3-phosphate oxidase are

Methods in Enzymology, Volume 571
ISSN 0076-6879
http://dx.doi.org/10.1016/bs.mie.2016.01.022

required for lipid analysis in a cascade reaction, and we describe the co-immobilization of these three enzymes on nanocomposites of zinc oxide nanoparticles (ZnONPs)—chitosan (CHIT) and gold nanoparticles-polypyrrole-polyindole carboxylic acid (AuPPy-Pin5COOH) which are electrodeposited on Pt and Au electrodes, respectively. The kinetic properties and analytes used for amperometric determination of TG are fully described for others to practice in a trained laboratory. Cyclic voltammetry, scanning electron microscopy, Fourier transform infra-red spectra, and electrochemical impedance spectra confirmed their covalent co-immobilization onto electrode surfaces through glutaraldehyde coupling on CHIT-ZnONPs and amide bonding on AuPPy/Pin5COOH. The combined activities of co-immobilized enzymes was tested amperometrically, and these composite nanobiocatalysts showed optimum activity within 4–5 s, at pH 6.5–7.5 and 35 °C, when polarized at a potential between 0.1 and 0.4 V. Co-immobilized enzymes showed excellent linearity within 50–700 mg/dl of the lipid with detection limit of 20 mg/dl for triolein. The half life of co-immobilized enzymes was 7 months, when stored dry at 4 °C which is very convenient for practical applications. Co-immobilized biocatalysts measured triglycerides in the sera of apparently healthy persons and persons suffering from hypertriglyceridemia, which is recognized as a leading cause for heart disease. The measurement of serum TG by co-immobilized enzymes was unaffected by the presence of a number of serum substances, tested as potential interferences. Thus, co-immobilization of enzymes onto aggregates of NPs resulted in improved performance for TG analysis.

1. INTRODUCTION

Triglycerides (TGs) are esters of glycerol and fatty acids in a stoichiometric molar ratio of 1:3, as the very name implies. These are the major components of very low-density lipoproteins (VLDL) and chylomicrons, which are aggregates of TG, phospholipids, proteins, and cholesterol. These are two of the five major classes of lipoproteins that play a very important role in the metabolism as energy sources as well as transporters of dietary fat from the intestines to other parts of the body. Increased level of TGs in the blood stream (>190 mg/dl) leads to atherosclerosis which increases the risk of heart disease, coronary heart disease (CAD), and hypolipoprotenimia. Normally, serum TG level in healthy persons is in the range of 150–190 mg/dl. The increased level of TG in the range 200–500 mg/dl is an alarming situation, while the level >500 mg/dl is troublesome (Nelson, Cox, & Lehninger, 2000). Hence, reliable measurement of TG levels in serum is very important for public health and for diagnosis of heart disease. Among various methods available for TG determination, enzymatic colorimetric method is the most popular. The method involves

a cascade of three enzymic reactions followed by a color reaction where the end point provides quantitation of TG. The three major reactions of the assay are catalyzed by three different enzymes, lipase, glycerol kinase (GK), and glycerol-3-phosphate oxidase (GPO), which are shown below:

$$\text{Triglyceride} + 3H_2O \xrightarrow{\text{Lipase}} 3\,\text{fatty acid} + \text{glycerol}$$

$$\text{Glycerol} + \text{ATP} \xrightarrow[Mg^{2+}]{\text{GK}} \text{glycerol-3-phosphate} + \text{ADP}$$

$$\text{Glycerol-3-phosphate} \xrightarrow{\text{GPO}} \text{dihydroxyacetone phosphate} + H_2O_2$$

The color reaction is as following:

$$H_2O_2 + \text{DHBS} + \text{4-aminophenazone} \xrightarrow{\text{Peroxidase}} \text{quinoneimine (pink color)}$$

DHBS, 3,5 dichloro-2-hydroxybenzene sulfonic acid.

However, this enzymatic colorimetric method employing free/native enzymes is expensive, when employed for a large number of samples, due to the high cost of the enzymes needed, and they cannot be recycled readily. These enzymes have poor stability under the experimental conditions encountered in an ordinary laboratory and need to be purchased periodically. Attachment of enzymes onto an insoluble support not only provides their reusability but also realizes the extra stabilization rendered by the multipoint covalent attachment or multisubunit binding of the enzymes on solid supports. In some cases, we and others found that enzymes bound to nanosolids improve enzyme activity, specificity, and/or stability (Barbosa et al., 2015; Kazenwadel, Franzreb, & Rapp, 2015; Kumar & Chaudhari, 2000, 2002). In recent years, solid-bound enzymes have revolutionized the prospects of enzyme applications in industry, and rational design of the solid support has gained major attention. Earlier, the biocatalyst preparation methodology was more like hit-and-trial but a rational design of the surface of the nanoparticles and rational choice of the linkage chemistry have improved the success of the approach, drastically. The rational approach is made possible through intense activity in understanding how enzymes and nanosolids interact at the molecular level, and a number of research groups around the world have contributed to this important activity (Chowdhury, Stromer, Pokharel, & Kumar, 2012; Duff & Kumar, 2009; Mudhivarthi, Bhambhani, & Kumar, 2007; Novak et al., 2016). Enzyme immobilization can be defined as the confinement of enzyme molecules onto/within a

support/matrix physically or chemically or both, in such a way that it retains its full activity or most of its activity.

When a series of reactions are to be conducted, as in the case of TG analysis reaction cascade, co-binding of multiple enzymes on the same particle has significant kinetic advantages. In a cascade reaction, the product of one enzyme is the substrate for another, and when all required enzymes are on the same particle, then this intermediary product does not have to diffuse from one particle to another particle to find its corresponding enzyme in the cascade reaction. Therefore, the diffusion distance and time are considerably shortened and such a system is more efficient than a mixture of separately bound enzyme particles, where the intermediary products will have to diffuse from one particle to the next for the continuation of the reaction steps (Minakshi & Pundir, 2008a, 2008b). However, one disadvantage of such a communal enzyme-particle approach is that when one or more enzymes in the assembly are deactivated, the entire assembly is effected.

Of the different techniques available for immobilization such as adsorption, encapsulation, microencapsulation, cross-linking, metal chelation, ionic binding, covalent binding is preferred, as it avoids enzyme leaching, provides comparative stability, durability, reusability, and shelf life. Lipase, GK, and GPO have been co-immobilized onto various supports such as collagen (Winartasaputra, Kutan, & Cuilbault, 1982), alkyl amine glass beads (Kalia & Pundir, 2002), aryl amine glass beads (Kalia & Pundir, 2004) through covalent coupling, and to cellulose acetate (Minakshi & Pundir, 2008a, 2008b), polyvinylchloride (PVC) (Narang, Bhambi, Minakshi, & Pundir, 2010), and polyvinyl alcohol (PVA) (Pundir, Singh, Bharvi, & Narang, 2010) through adsorption. In contrast, intercalation of enzymes in the galleries of nanosheets was enhanced by tuning enzyme charge, and enzyme stability increased at an unprecedented 150-fold (Novak et al., 2016). Such rational design of the nanomaterials is of intense interest for making progress in the cascade reaction catalysis. In contrast, physical adsorption of the enzymes onto membranes has the risk of their leakage during the washing for reuse.

2. USE OF RATIONALLY DESIGNED NANOSCAFFOLDS FOR ENZYME BINDING

Materials when reduced down to 1–100 nm in one or more of their dimensions, exhibit drastic changes in their physical, chemical, optical, magnetic, or electrochemical properties, which lead to exciting applications in

bioscience, medicine, environmental science, and various industries. Different nanostructures have been synthesized such as nanoparticles (NPs), nanorods, nanotubes, nanofibers, nanospheres and nanofilms. Of these nanostructures, NPs and clusters of nanoparticles are most often employed for enzyme binding due to the possibility for rational control of the enzyme–solid interactions at these surfaces.

NPs can be organic, inorganic, or biological in nature, and this chapter focuses on zinc oxide nanoparticles (ZnONPs) which are potentially good nanomaterials for enzyme binding because of favorable properties such as their large surface area due to large volume to weight ratio, high catalytic efficiency, non-toxicity, chemical stability, strong adsorption ability, and high isoelectric point, pH 9.5. Nanoporous nature of the ZnONPs also enhances the active surface area for strong adsorption of biomolecules (Singh et al., 2007; Wang et al., 2006; Wei et al., 2006).

3. USE OF CHITOSAN FOR ENHANCING NANOPARTICLE SURFACE CHEMISTRY

Chitosan (CHIT) is an interesting biopolymer for the binding of a variety of biomolecules (including enzymes), because of excellent film-forming ability, high permeability, good mechanical strength, non-toxicity, biocompatibility, low cost, and easy availability. Moreover, chemical modification of the amino groups of CHIT provides hydrophilic environment, which may be necessary for the retention of the native-like structures of most biomolecules (Jiang et al., 2007; Liao, Lin, & Wu, 2005).

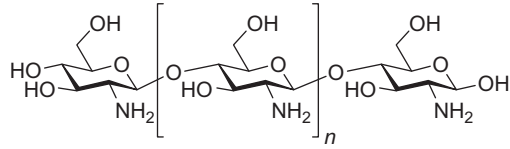

Chemical structure of chitosan *Source: Wikipedia.*

Likewise, gold polypyrrole (AuPPy) nanocomposites have a remarkable property. They adhere easily to Au electrodes and show a better electrocatalytic reduction than bare Au electrode. Further, AuNPs AuPPy nanocomposites help in faster electron transfer to the electrodes. Poly (indole-5-carboxylic acid) (Pin5COOH) not only facilitates the electron transfer between enzymes and electrode but also provides free COOH groups for the covalent binding with $-NH_2$ groups on the surface of enzymes.

This chapter describes the co-immobilization of lipase, GK, and GPO onto nanocomposites of CHIT-ZnONPs electrodeposited that are onto Pt and AuPPy–Pin5COOH electrodeposited onto Au electrodes. The kinetic properties and applications of these electrodes in the construction of amperometric TG biosensors are examined and improved analytic performance has been noted (Narang & Pundir, 2011; Narang, Chauhan, Rani, & Pundir, 2012).

4. EXPERIMENTAL

4.1 Combined Assay of Mixture of Free/Native Lipase, GK and GPO

4.1.1 Preparation of Mixture of Enzymes

Materials: Lipase (from porcine pancreas), glycerol kinase (GK, from *Cellulomonas*), glycerol-3-phosphate oxidase (GPO, from *Aerococcus viridans*), $MgCl_2$, ATP, potassium ferrocyanide, 4-aminophenazone, 3,5 dichloro-2-hydroxybenzene sulfonic acid (DHBS), triolein solution, and Triton X-100.

Equipment: UV–vis spectrophotometer.

Dissolve 2.0 mg of lipase (from porcine pancreas; 40–70 U/mg) + 1.0 mg GK (from *Cellulomonas* sp; 25–75 U/mg) + 0.1 mg GPO (from *Aerococcus viridans*; 113 U/mg) into 1.0 ml of 0.02 *M* sodium phosphate buffer (PB), pH 7.0, of 50–100 units of each of the three enzymes in the mixture and store at 4 °C until use.

4.2 Combined Assay of Enzymes

The combined assay of mixture of lipase, GK and GPO in solution is carried out in a 15-ml conical flask wrapped with a black paper, as described previously (Fossati & Prencipe, 1982). First, prepare a reaction mixture consisting of 0.54 μmol $MgCl_2$, 0.63 μmol ATP, 1.0 μmol potassium ferrocyanide, 0.27 μmol 4-aminophenazone, 1.0 μmol DHBS, and 1.0 μmol of Triton X-100 in a total volume of 1 l of 0.1 *M* PB, pH 7.0. To 900 μl of this reaction mixture, add 50 μl of enzyme mixture and preincubate at 37 °C for 5 min. To start the reaction, add 50 μl of 22.6 m*M* triolein solution (commercially available at a concentration of 200 mg/dl in the kit for enzymic colorimetric determination for TGs supplied by Span Diagnostics, Surat, Gujarat, India) to this mixture and incubate it at 37 °C for 15 min. Read absorbance at 510 nm (A_{510}) of the reaction mixture against the control/blank in Spectronic $20D^+$ (Thermo Scientific, USA) and calculate μmol of H_2O_2 generated, using a standard curve

generated with known concentrations of H_2O_2. The unit activity of mixture of enzyme is expressed as μmol H_2O_2 generated in the assay/min/ml of mixture of enzymes.

4.2.1 Covalent Co-Immobilization of Lipase, GK, and GPO onto Nanocomposite of ZnONPs/CHIT Electrodeposited onto Pt Electrode

4.2.1.1 Preparation of ZnONPs

Materials: Zinc nitrate ($Zn(NO_3)_2 \cdot 4H_2O$), NaOH, and ethanol.

Equipment: Magnetic stirrer.

To synthesize ZnONPs, prepare 0.9 *M* sodium hydroxide (NaOH) solution and 0.45 *M* zinc nitrate ($Zn(NO_3)_2 \cdot 4H_2O$) in double distilled water (DW). Heat NaOH solution (100 ml) at 55 °C and then add 50 ml $Zn(NO_3)_2$ solution dropwise (slowly for 40 min) into hot NaOH solution, under high-speed stirring on a hot plate (Remi, New Delhi, India). Seal the beaker during this process for 2 h, clean the precipitated ZnONPs with DW, until the pH of wash is 7.0, followed by washing once with 10 ml ethanol, and then air dry in hot air oven (NSW, New Delhi) at 60 °C (Lata, Batra, Singala, & Pundir, 2013).

4.2.1.2 Characterization of ZnONPs

Techniques: Transmission electron microscopy and powder XRD.

Before characterization of NPs, sample preparation is required. In case of transmission electron microscopy (TEM), prepare NP suspension in ethanol by sonication in Misonix ultrasonic liquid processor (XL 2000 series, Newtown City, USA) for 15 min and for X-ray diffraction (XRD), grind NPs powder in pestle and mortar until it becomes a fine powder and press it into sample holder of X-ray diffractometer (122 Rigaku, D/Max2550, Tokyo, Japan) to get a smooth plane surface for XRD study. Two techniques are employed to characterize the following properties of ZnONPs.

4.2.1.3 Shape and Size

TEM images of ZnONPs taken in transmission electron microscope (JEOL 2100 F, USA) showed their spherical structure with average size of 50 nm but their aggregates had a flower-like structure (Fig. 1) and XRD pattern shows peaks which are consistent with the peaks of wurtzite ZnO (JCPDS card No. 36-1451, $a = 3.249$ Å, $c = 5.206$ Å) with high crystallinity (Fig. 2). Furthermore, no other characteristic peaks are observed, revealing no impurities in the samples (Narang & Pundir, 2011).

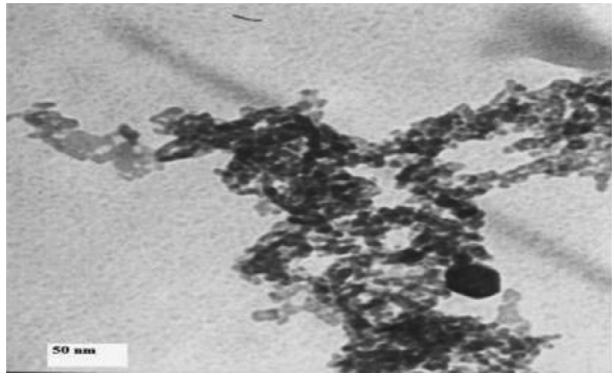

Figure 1 Transmission electron microscopic (TEM) image of ZnONPs. *Reprinted from Narang and Pundir (2011), with permission from Elsevier.*

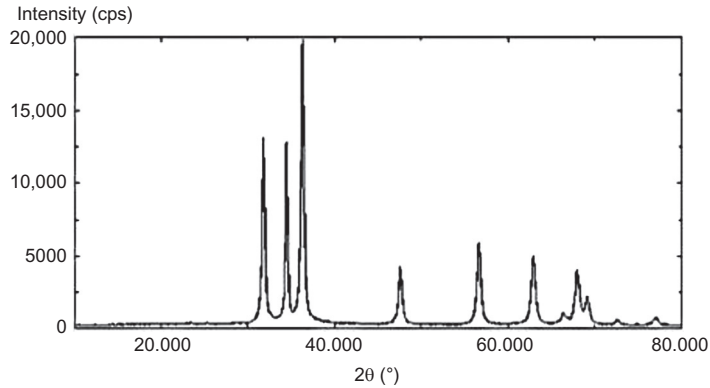

Figure 2 X-ray diffraction (XRD) pattern of ZnONPs. *Reprinted from Narang and Pundir (2011), with permission from Elsevier.*

4.2.1.4 Preparation of ZnONPs-CHIT Composite

Equipment: Ultrasonicator, scanning electron microscope, and FTIR spectrophotometer.

Disperse ZnONP powder (5 mg) into transparent CHIT solution (0.5 g of CHIT/10 ml of 0.05 *M* acetate buffer solution, pH 5.0) and keep it overnight at room temperature, followed by magnetic stirring for 30 min to mix the contents, and then sonicate it for about 1 h at room temperature. The hybrid nanocomposite of ZnO NP-CHIT is formed overnight, which is confirmed by comparing its scanning electron microscopic (SEM) images, taken in scanning electron microscope (Joel JSM 6510, Japan) and Fourier transform infra-red (FTIR) spectra taken in FTIR spectrophotometer (iS10,

Thermo Scientific, USA) and compared with the corresponding data obtained from CHIT control samples (Narang & Pundir, 2011).

4.2.1.5 Deposition of ZnO NPs-CHIT Composite onto Pt Electrode

Deposit nanocomposite film onto Pt electrode (PtE) by dipping the electrode into solution of hybrid nanocomposite of ZnONPs-CHIT overnight. Activate hybrid nanocomposite film by dipping the modified electrode into 2.5% glutaraldehyde in 0.02 *M* PB, pH 7.0, and keep it for 2 h at room temperature. Remove this activated electrode from buffer and wash it thoroughly with 0.02 *M* PB, pH 7.0, until the pH of wash is neutral and apply it onto Pt electrode (surface area of 0.25 cm^2) (Narang & Pundir, 2011).

4.2.1.6 Co-Immobilization of Lipase, GK, and GPO onto ZnO NPs-CHIT/PtE

Dip the nanocomposite film modified Pt electrode into 1 ml mixture of lipase, GK, and GPO dissolved in 0.02 *M* PB, pH 7.0, and keep it overnight at 4 °C for the covalent immobilization. Wash the enzyme electrode with DW for number of times, followed by 50 m*M* PB, pH 7.0, to remove unbound enzyme, until the pH of wash is 7.0. Keep the enzyme electrode, i.e., enzymes/nanoZnO-CHIT/Pt electrode undisturbed for about 12 h at 4 °C (Narang & Pundir, 2011).

4.2.1.7 Chemistry of Immobilization of Enzymes on ZnONPs/CHIT Nanocomposite

The covalent co-immobilization of enzymes onto ZnONPs-CHIT composite involves the activation of CHIT of ZnONPs-CHIT nanocomposite by glutaraldehyde (a bifunctional reagent, a powerful cross-linker, and a versatile tool in covalent immobilization of enzymes) and then interaction between activated CHIT and enzymes through Schiff base as following:

$$\underset{\text{Chitosan}}{\text{CHIT-NH}_2} + \text{OHC-(CH}_2)_3\text{-CHO} \rightarrow \text{CHIT-NH} = \underset{\text{Glutaraldehyde}}{\text{CH-(CH}_2)\text{-CHO}} + \text{H}_2\text{O}$$

$$\text{CHIT-NH} = \underset{\text{Enzyme}}{\text{CH(CH}_2)_3}\text{-CHO} + \text{NH}_2\text{-E}$$

$$\rightarrow \underset{\text{Immobilized enzymes}}{\text{CHIT-NH} = \text{CH-(CH}_2)_3 - \text{CH} = \text{NH-E}} + \text{H}_2\text{O}$$

The steps involved in the binding of enzymes onto nanocomposite of CHIT-ZnONPs are shown in Fig. 3.

Tip: The Schiff base thus formed is prone to hydrolysis unless reduced with a reagent such as sodium borohydride to form the corresponding amine.

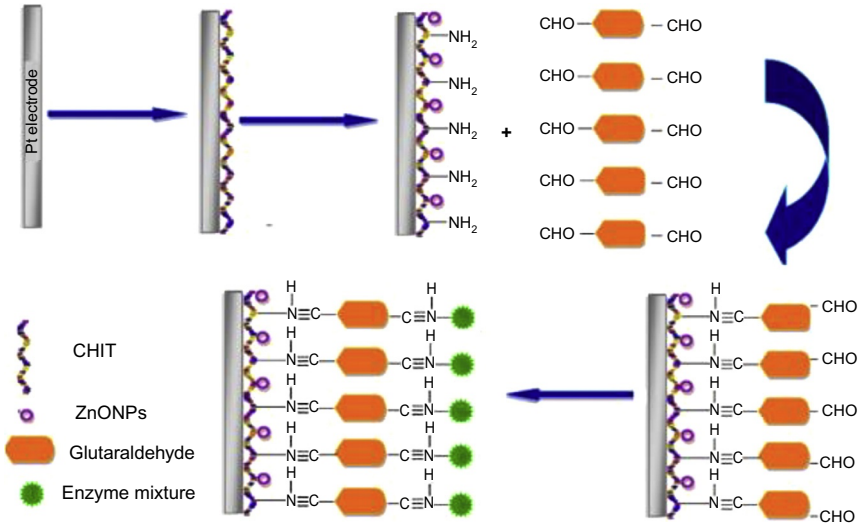

Figure 3 Schematic representation of ZnONPs/CHIT electrode preparation and immobilization of enzymes on it. Step 1+Step 2: Uniform spreading of chitosan solution containing ZnONPs onto Pt electrode; Step 3: Activation of CHIT/ZnONPs/PtE; Step 4: Covalent co-immobilization of mixture of lipase, GK, and GPO onto activated electrode. *Reprinted from Narang and Pundir (2011), with permission from Elsevier.*

4.2.2 Covalent Co-Immobilization of Lipase, GK, and GPO onto Nanocomposite Film of Pin5COOH/AuPPy Electrodeposited onto Au Electrode

4.2.2.1 Construction of Gold Polypyrrole (AuPPy) Nanocomposite

Materials: Pyrrole, $HAuCl_4$, and cetyl trimethyl ammonium bromide (CTAB).

A nanocomposite of AuPPy is prepared by direct redox reaction between pyrrole monomers and $HAuCl_4$ as described (Miao, Wu, Chen, Liu, & Qiu, 2008). Mix 10 µl pyrrole into 2 ml of 0.5 *M* H_2SO_4 containing 10 m*M* CTAB and then add 10 µl of 2 m*M* $HAuCl_4$ aqueous solution dropwise and stir overnight on a magnetic stirrer (Remi, New Delhi). The appearance of transparent light yellow color confirms the formation of stably dispersed AuPPy colloid (Narang et al., 2012).

4.2.2.2 TEM Characterization of AuPPy Nanocomposite

TEM is employed to confirm the formation of AuPPy nanoparticles. The TEM image of this nanocomposite shows spherical shape with diameter of 20 nm. In addition to these, small submicron particles are dispersed on the surface; as a result, large agglomerates are seen in the image, which confirm the formation of nanocomposite of AuPPy (Fig. 4) (Narang et al., 2012).

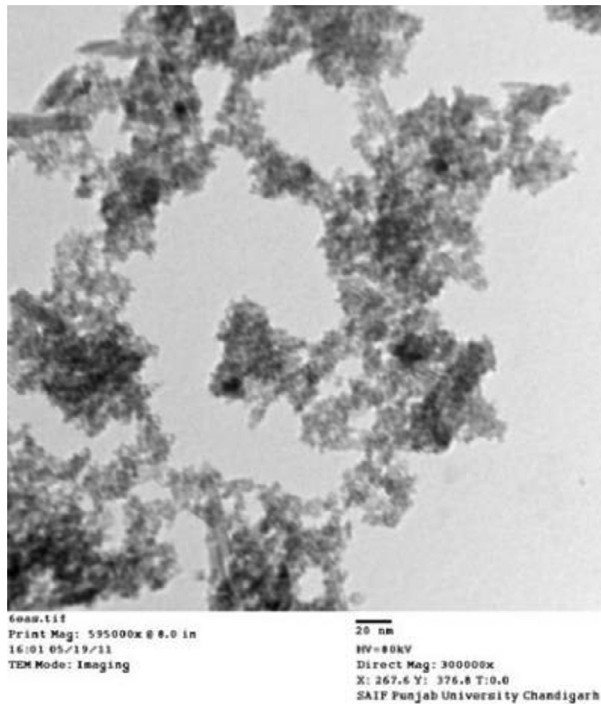

Figure 4 Transmission electron microscopic (TEM) image of AuPPy. *Reprinted from Narang et al. (2012), with permission from Elsevier.*

4.2.2.3 Preparation of Nanocomposites of AuPPy and Pin5COOH

The nanocomposite of AuPPy and Pin5COOH is prepared as described, (Vu et al., 2005) with some modification. To prepare it, add $FeCl_3$ (4.5 g) to a mixture of 1.0 ml AuPPy suspension and 1.0 ml indole monomers (5.0 mg in 20.0 ml DW) under continuous stirring for 2 h, wash the particles of nanocomposite with DW, filter, extract them (in ethanol) for 10 h and then dry at 50 °C.

4.2.2.4 Electrodeposition of Pin5COOH/AuPPynano-Composite onto Au Electrode

Technique: Cyclic voltammetry.

Electropolymerization/deposition of nanocomposite of Pin5COOH/AuPPy onto Au electrode from acetonitrile solution is carried out as follow: Polish an Au (1.5 cm × 0.05 cm) electrode with alumina powder followed by cyclic voltammetry in the potential range, from 0.0 to 0.6 V versus Ag/AgCl, at a scan rate 20 mV/s. Immerse the cleaned Au electrode in

25 ml acetonitrile containing 0.1 g nanocomposite and then apply 10 polymerization cycles in the potential range from 0.0 to 0.6 V and back to 0.0 V at a scan rate of 20 mV/s. After electrodeposition/polymerization, wash the electrode carefully with acetonitrile and finally with DW (Barlett, Dawnson, & Farrington, 1992).

4.2.2.5 Co-Immobilization of Lipase, GK, and GPO onto Pin5COOH/AuPPy/AuE (Au Electrode)

Covalent immobilization of a mixture of lipase, GK, and GPO onto nanocomposite of Pin5COOH/AuPPy/AuE is carried out as follow: Add 20 μl mixture of enzymes on the surface of this Pin5COOH/AuPPy modified AuE and keep it at 4 °C. After 10 min, wash the electrode with DW and use it for electrochemical measurements (Narang et al., 2012).

4.2.2.6 Chemistry of Immobilization of Enzymes on Pin5COOH/AuPPy Nanocomposite

The chemical reaction involved in the co-immobilization of enzymes onto Pin5COOH/AuPPy nanocomposite includes the covalent cross-linking between $-NH_2$ groups on surface of enzyme and –COOH group of Pin5COOH/AuPPy nanocomposite through amide linkage as follow:

$$\underset{\text{Enzyme}}{\text{E-NH}_2} + \text{HOOC-5-Pin/AuPPy nanocomposite} \rightarrow \underset{\text{Immobilized enzyme}}{\text{E-NH-CO-5-Pin/AuPPy}} + \text{H}_2\text{O}$$

The steps involved in immobilization of enzymes on nanocomposite of AuPPy/Pin5COOH are shown in schematic diagram in Fig. 5.

4.2.2.7 Confirmation of Co-Immobilization of Enzymes

The co-immobilization of enzymes onto nanocomposites of ZnONPs-CHIT/Pt and AuPPy/Pin5COOH/Au is confirmed by high-resolution SEM, electrochemical impedance spectroscopic spectra (EIS), FTIR spectra, and cyclic voltammetry (CV) (Autolab, Eco Chemie, The Netherlands. Model: AUT83785) as follow.

SEM: Figure 6A–D shows SEM images of bare Pt electrode, CHIT/Pt, ZnONPs/CHIT/Pt, and enzymes/CHIT/ZnONPs/Pt. The SEM image of bare Pt electrode displayed the homo granular space (Fig. 6A), while CHIT deposited Pt electrode has rough surface due to deposition of CHIT film (Fig. 6B). The ZnONPs/CHIT/Pt electrode showed the dispersed ZnONPs in chitosan matrix (Fig. 6C). Immobilization of enzymes onto

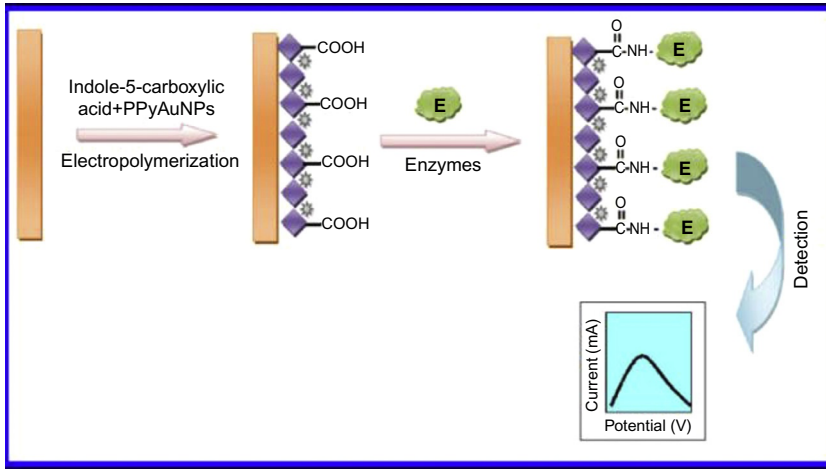

Figure 5 Schematic representation of AuPPy/Pin5COOH electrode preparation and chemical reactions involved in covalent co-immobilization of enzymes (⚙, AuPPy; ◆, Pin5COOH). *Reprinted from Narang et al. (2012), with permission from Elsevier.*

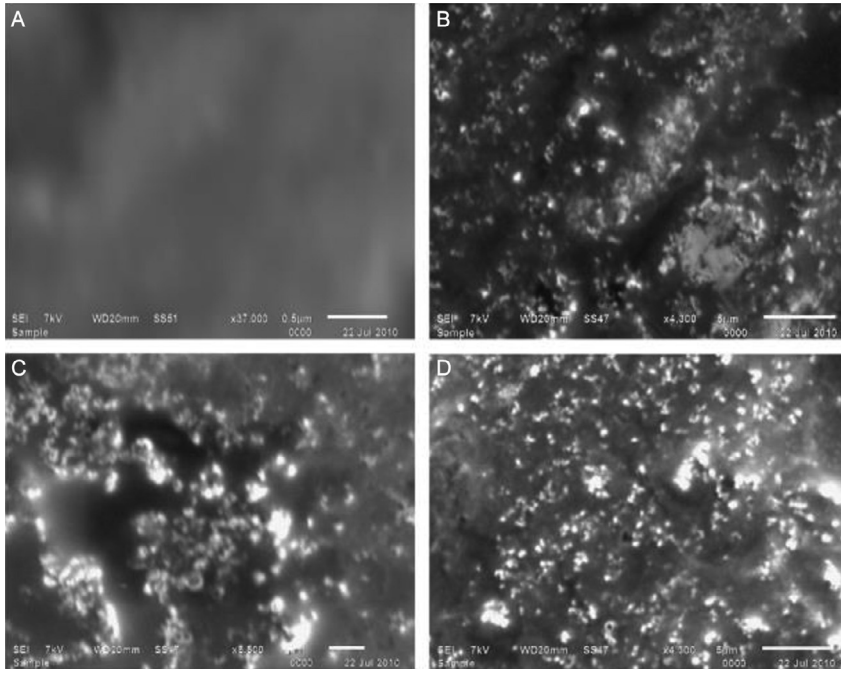

Figure 6 Scanning electron microscopic (SEM) images of (A) bare electrode, (B) CHIT/ electrode, (C) ZnONPs/CHIT/electrode, and (D) enzymes/ZnONPs/CHIT/electrode. *Reprinted from Narang and Pundir (2011), with permission from Elsevier.*

the granular morphology of ZnONPs/CHIT nanocomposite changed into the regular form to confirm the interaction between the nanocomposite and enzymes (Fig. 6D) (Narang & Pundir, 2011).

Figure 7A–C exhibits the SEM images of bare Au electrode, Pin5COOH/AuPPy/Au electrode, and enzymes/Pin5COOH/AuPPy/Au

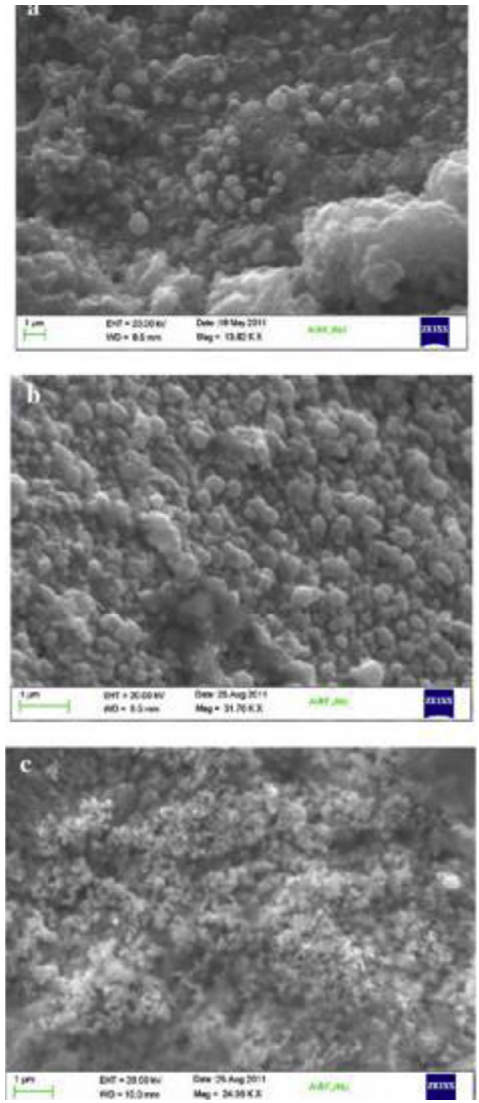

Figure 7 Scanning electron microscopic (SEM) images of (A) bare electrode, (B) Pin5COOH/AuPPy/Au, and (C) enzyme/Pin5COOH/AuPPy/Au. *Reprinted from Narang et al. (2012), with permission from Elsevier.*

electrode The surface morphologies of bare (Au) electrode show smooth surface (Fig. 7A), nanocomposite modified Au electrode exhibit granular morphology with heterogeneous roughness of Pin5COOH/AuPPy/Au electrode depicting the dispersed NPs in Pin5COOH matrix (Fig. 7B), while the enzymes/Pin5COOH/AuPPy/Au electrode, has the granular morphology of Pin5COOH/AuPPy changed into the regular form, due to the co-immobilization/interaction between Pin5COOH-AuPPy and enzymes (Fig. 7C) (Narang et al., 2012).

EIS spectra: Electrochemical impedance spectra also known as dielectric spectroscopy measures the dielectric properties of a medium as a function of frequency. Figure 8 shows spectra of (■) CHIT/Pt electrode, (•) nanoZnO-CHIT/Pt electrode, and (▲) enzymes/nanoZnO-CHIT/Pt electrode. The charge transfer process in enzymes/nanoZnO-CHIT/Pt electrode is studied by monitoring charge transfer resistance (R_{ct}) at the electrode and electrolyte interface. The R_{ct} value depends on the dielectric and insulating features at the electrode/electrolyte interface. The R_{ct} values for the CHIT/Pt, nanoZnO-CHIT/Pt, and enzymes/nanoZnO-CHIT/Pt electrodes as calculated from semicircle of EIS spectra are 6.68×10^2, 4.47×10^2, and 22.38×10^2 **Ω**, respectively. The electron transfer via redox couple is hindered by the presence of enzymes on electrode surface. The increased R_{ct} value of enzymes/nanoZnO-CHIT/Pt electrode is due to the fact that most biological molecules, including enzymes, are poor electrical conductors at low frequencies (at least <10 KHz) and cause hindrance to the electron transfer (Narang & Pundir, 2011).

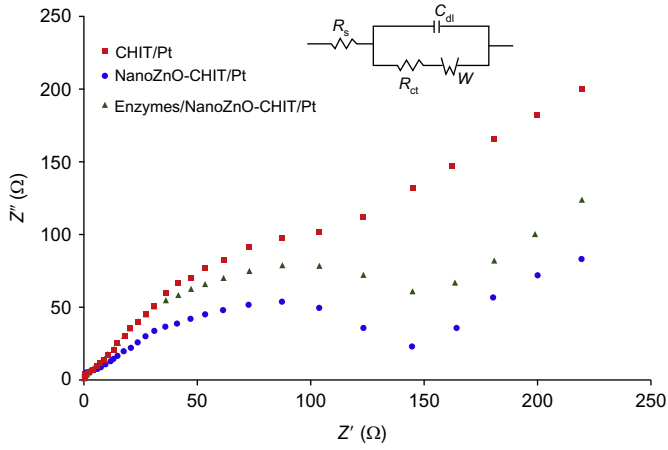

Figure 8 Electrochemical impedance spectra (EIS) of (■) CHIT/Pt, (•) ZnONPs/CHIT/Pt, and (▲) enzymes/ZnONPs/CHIT/electrode. *Reprinted from Narang and Pundir (2011), with permission from Elsevier.*

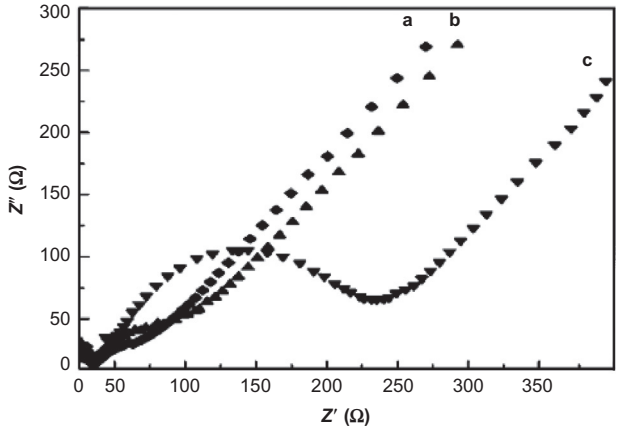

Figure 9 Electrochemical impedance spectra (EIS) of (a) AuPPy/Au, (b) Pin5COOH/AuPPy/Au, and (c) enzyme/Pin5COOH/AuPPy/Au. *Reprinted from Narang et al. (2012), with permission from Elsevier.*

Figure 9a–c shows EIS of (a) AuPPy/Au electrode, (b) Pin5COOH/AuPPy/Au electrode, and (c) enzymes/Pin5-COOH/AuPPy/Au electrode. The R_{ct} values for the AuPPy/Au electrode, Pin5-COOH/AuPPy/Au electrode, and enzymes/Pin5COOH/AuPPy/Au electrode are 90, 60, and 225 **Ω**, respectively. The increased R_{ct} value of enzymes/Pin5-COOH/AuPPy/Au electrode is due to the immobilization of enzymes onto Pin5COOH/AuPPy/Au surface (Narang et al., 2012).

FTIR spectra: The FTIR spectra of (i) CHIT/Pt, (ii) ZnONPs-CHIT/Pt electrode, and (iii) enzymes/ZnONPs-CHIT/Pt electrode are compared in Fig. 10. The spectrum of CHIT shows characteristic absorption band of aminosaccharide at 3421, 2811, and 1647 cm^{-1}, due to overlapping of –OH and $–NH_2$ stretchings, CH_2 stretching, and C–O stretching, respectively. CHIT-ZnONPs composite films show an additional peak at 492 cm^{-1} corresponding to ZnONPs, which confirms the formation of ZnONPs-CHIT hybrid. Enz/CHIT-ZnONPs/electrode shows broadening of the peak at 3264 and 1653 cm^{-1}, due to the addition of carbonyl groups of glutaraldehyde and amino groups on the surfaces of enzymes, bound onto ZnONPs-CHIT film (Narang & Pundir, 2011).

Figure 11a and b shows the FTIR spectra for Pin5COOH/AuPPy/Au electrode (curve a) and enzymes/Pin5COOH/AuPPy/Au electrode (curve b). The spectrum associated with the oxidized Pin are characterized by a very large adsorption band located in the spectral domain between 3700 and 3100 cm^{-1}, which is characteristic of –OH groups belonging to

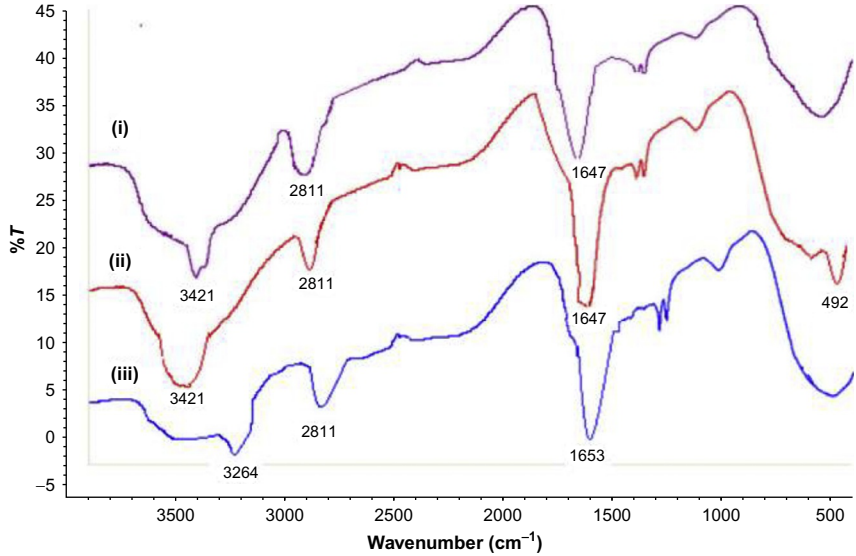

Figure 10 FTIR spectra of (i) CHIT/Pt, (ii) ZnONPs/CHIT/Pt, (iii) enzymes/ZnONPs/CHIT/Pt. *Reprinted from Narang and Pundir (2011), with permission from Elsevier.*

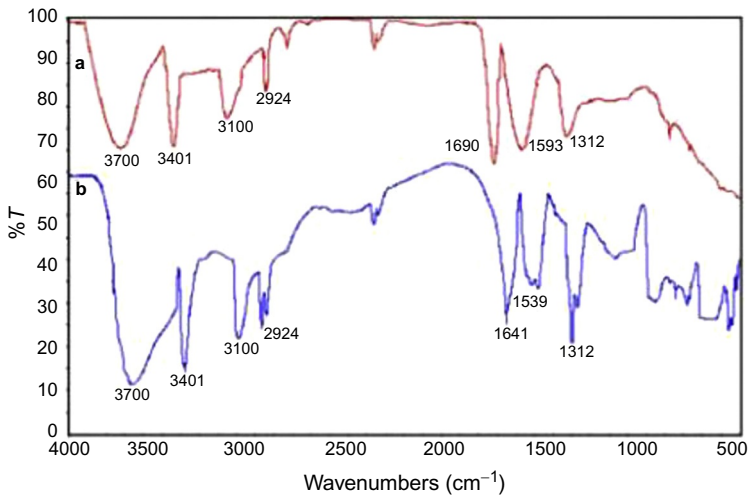

Figure 11 FTIR spectra of (a) Pin5COOH/AuPPy/Au and (b) enzyme/Pin5COOH/AuPPy/Au. *Reprinted from Narang et al. (2012), with permission from Elsevier.*

residual water molecules trapped in the polymer matrix as well as water molecules absorbed in Pin. The peaks at 3401, 2924, 1593, and 1312 cm^{-1} are due to –N–H stretching, –C–H (aromatic) stretching, C–C stretching, and C–N stretching (between two indole units),

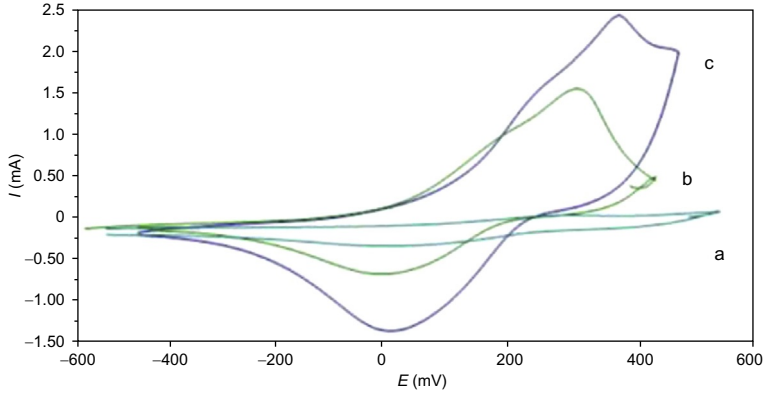

Figure 12 Cyclic voltammograms (a) CHIT/Pt, (b) ZnONPs/CHIT/Pt, (c) enzymes/ZnONPs/CHIT/Pt. *Reprinted from Narang and Pundir (2011), with permission from Elsevier.*

respectively. A sharp absorption peak at 1690 cm^{-1} is due to the attachment of –COOH group onto the indole. FTIR spectrum of enzymes/Pin5COOH/AuPPy/Au (curve b), confirm the covalent immobilization of enzyme as indicated by the appearance of additional absorption bands at 1641 and 1539 cm^{-1} assigned to the carbonyl stretch (amide I band) and –N–H bending (amide II band), respectively (Narang et al., 2012). Further, enzyme attachment to the nanocomposites is confirmed when the enzymes are not released after washing of the enzyme electrodes with detergents or guanidine hydrochloride solutions.

CV: Figure 12a–c shows the cyclic voltammograms for CHIT/Pt electrode, ZnO-CHIT/Pt electrode, and enzymes/nanoZnO-CHIT/Pt electrode in PB (50 m*M*, pH 7.0, plus 0.9% NaCl) containing $[Fe(CN)_6]^{3}]^{4-}$ (5 m*M*) recorded at different scan rates (10–100 mVs^{-1}), respectively. The anodic potential was shifted toward positive side and the cathodic peak potential shifted in the reverse direction. The redox potential of nanoZnO-CHIT electrode shifted toward the higher side than that of the pure CHIT film, which is due to the incorporation of ZnONPs in the film. The nanoZnO-CHIT nanocomposite electrode appears to provide a biocompatible environment to the enzymes, and ZnONPs act as electron mediators, resulting in an accelerated electron transfer between enzymes and electrode (Narang & Pundir, 2011).

Cyclic voltammograms for AuPPy/Au electrode, Pin5COOH/AuPPy/Au electrode, and Enz/Pin5COOH/AuPPy/Au electrode in presence of 20 m*M* triolein in PBS (0.1 *M*, pH 7.5) are shown in Fig. 13. No peak is observed in case of the bare electrode. The polymer showed two

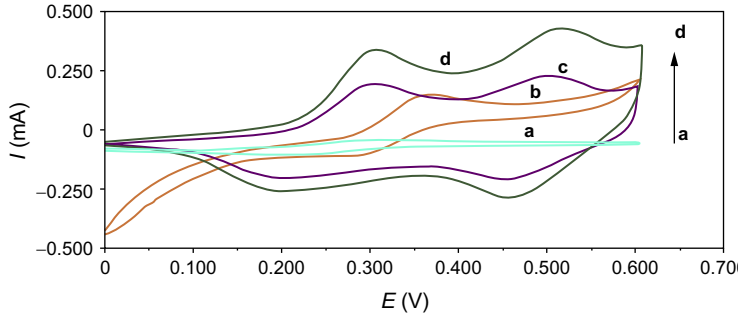

Figure 13 Cyclic voltammograms (CV) of (a) bare electrode, (b) AuPPy/Au, (c) Pin5COOH/AuPPy/Au, and (d) enzyme/Pin5COOH/AuPPy/Au (Narang et al., 2012). *Reprinted from Narang et al. (2012), with permission from Elsevier.*

characteristic peaks, which are the known oxidation and reduction peaks observed in acetonitrile. The nanocomposite provided a conductive path for electron transfer and promoted electron transfer at lower potentials (Narang et al., 2012).

4.3 Kinetic Properties of Co-Immobilized Lipase, GK, and GPO

4.3.1 Optimum pH

Most enzymes have highest activity around an optimum pH (or pH range) and therefore, at other pH values, enzymatic activity decreases substantially. Certain pH values might promote dissociation of multimeric enzymes and decrease their activities. Amino acid side chains in the active site may act as weak acids or/and bases and hence, the catalytic activity depends on the pH of the medium. The pH range over which enzyme activity changes substantially can provide clues as to the type of amino acid residues involved in the catalytic cycle. Binding of the enzyme on a nanosurface might alter the local pH of the medium surrounding the bound enzyme, and hence, this can influence the pH optimum for the bound enzyme to be different from that of the soluble enzyme. The ionized side chains of proteins may also play an important role in the interactions that maintain enzyme/protein structure. To study optimum pH for the activity of the bound enzyme, 0.1 *M* sodium phosphate buffer was used, which was adjusted to have the pH in the range of 6.0–8.0 at an interval of 0.5. The optimal pH of the mixture of the three soluble enzymes are examined here (pH 7.2) which is increased to 7.5 when bound to ZnONPs/CHIT/Au electrode (Fig. 14) (Narang & Pundir, 2011) and the pH optimum decreased to 6.5 upon binding to AuPPy/Pin5-COOH/Pt electrode (Narang et al., 2012) (Table 1).

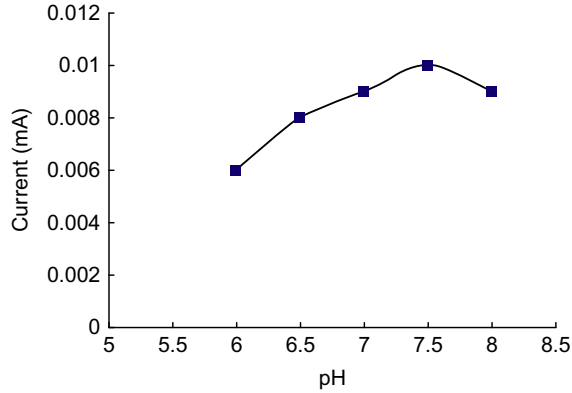

Figure 14 Effect of pH on enzymes/ZnONPs/CHIT/Pt electrode. *Reprinted from Narang and Pundir (2011), with permission from Elsevier.*

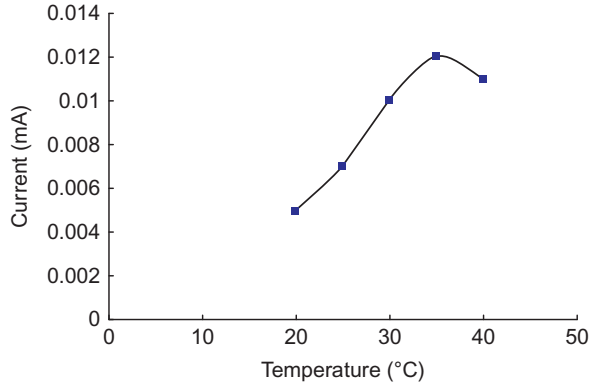

Figure 15 Effect of temperature on enzymes/ZnONPs/CHIT/Pt modified electrode. *Reprinted from Narang and Pundir (2011), with permission from Elsevier.*

4.3.2 Optimum Temperature

In addition to the pH optimum, most enzymes may also have an optimum temperature for maximal activity. The optimum temperature of the both samples of the bound enzymes is 35 °C and this is a small increase when compared to that of the corresponding free enzymes. For example, an increase of 2 °C for lipase when co-immobilized with GK and GPO onto the nanosupport (Fig. 15) (Narang & Pundir, 2011; Narang et al., 2012), but could be well within the experimental error. Co-immobilized enzymes show enhanced thermostability when compared to those of the corresponding free enzymes (data not shown). This increased thermal stability could be due to intramolecular covalent cross-linkages with the support

(nanocomposite), which prevent conformational changes in the enzyme at higher temperature, and thus inhibits the enzyme deactivation (Table 1).

4.3.3 Response Time

Another important characteristic for most biocatalysts is their response time, which is defined as the time needed for an enzyme to produce an electrochemical response due to the product generated during the catalytic cycle. Thus, not only the catalytic cycle is involved but the generation of the electrochemical signal from the product at appropriate potential is reflected in the response time. When lipase, GK, and GPO are bound to CHIT/ZnO nanofilm, the current is produced within 6 s (Fig. 16) (Narang & Pundir, 2011). However, when these enzymes are immobilized on AuPPy/Pin5COOH, the response time was 4 s (Narang et al., 2012) which is slightly faster than that of the mixture of the free enzymes (15 min). The later result could be due to faster diffusion of the product to the electrode or that the free enzyme has to diffuse to the electrode surface for the chemistry to occur. Thus, electrode-bound enzymes could be substantially more advantageous for biocatalysis applications (Table 1).

4.3.4 Working Range/Linearity

The concentration range over which the substrate is consumed and product produced linearly is called the working range and it is an important parameter for biocatalysis, as this allows for the most efficient use of the biocatalyst. Above or below this range, there may be excess or insufficient amount of the substrate to take full advantage of the biocatalyst capacity. When lipase, GK,

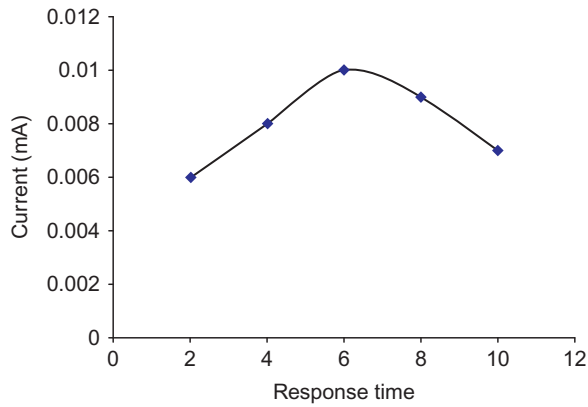

Figure 16 Response time for enzymes/ZnONPs/CHIT/Pt modified electrode. *Reprinted from Narang and Pundir (2011), with permission from Elsevier.*

and GPO were immobilized on CHIT/ZnO nanofilm, the working range has been found to be between 50 and 650 mg/dl (Narang & Pundir, 2011). When the enzymes were immobilized on AuPPy/Pin5COOH nanocomposite, this range was 50–700 mg/dl (Narang et al., 2012). These are comparable to that of the mixture of free enzymes (40–400 mg/dl) (Table 1).

4.3.5 Storage Stability

The storage stability is the time during which enzyme can be stored without considerable loss in its activity, and this is another important criterion for the practical application of biocatalyst. Longer the storage time, the greater the utility of the biocatalytic preparation. The mixture of lipase, GK, and GPO were stored at 4 °C for 6 months, while co-immobilized enzymes on CHIT/ZnONPs (Narang & Pundir, 2011) and AuPPy/Pin5COOH nanocomposite (Narang et al., 2012) have been stored at 4 °C for 7 months without considerable loss in their activities, which is only slightly longer than that of the mixture of free enzymes (6 months) (Table 1).

Table 1 A Comparison of Kinetic Properties of Lipase, Glycerol Kinase, and Glycerol-3-Phosphate Oxidase Co-Immobilized onto Two Different Nanocomposites Electrodeposited on Metal Electrode

Property	Mixture of Free Enzyme	Enz/CHIT/ZnONPs/Pt (Narang & Pundir, 2011)	Enz/Pin5COOH/AuPPyNPs/Au (Narang et al., 2012)
Type of electrode	–	Pt	Au
Method of immobilization	–	Covalent	Covalent
Type of bonding	–	Schiff base	Amide linkage
Optimum pH	7.2	7.5	6.5
Optimum temperature (°C)	37	35	35
Potential for maximum current (V)	–	0.4	0.1
Detection limit for triolein (mg/dl)	–	20	20
Linear range for triolein (mg/dl)	40–400	50–650	50–700
Response time	15 min	6 s	4 s
Storage stability (months)	6	7	7

CHIT, Chitosan; ZnONPs, zinc oxide nanoparticles; Pin5COOH, poly (indole-5-carboxylic acid); AuPPy, gold polypyrrole nanocomposite.

4.4 Application of Co-Immobilized Lipase, GK, and GPO onto Nanomaterials

The co-immobilized lipase, GK, and GPO onto nanomaterials were tested for the construction of improved amperometric biosensor for the detection of TGs in biological fluids. A biosensor is defined as an analytical device which consists of a biological sensing element connected to a transducer which converts biological response into a measurable signal. For practical applications, the magnitude of the signal should be directly proportional to the concentration of analyte over sufficient concentration range. A biosensor has the advantage over other analytical devices in terms of their simplicity, rapidity, sensitivity, and specificity. Among the various types of biosensors known, amperometric biosensors are quite common, which measure current, against the concentration of the analyte.

4.4.1 Principle of Amperometric TG Biosensor

In amperometric TG biosensor, H_2O_2 is generated from TG by the combined reaction of lipase, GK, and GPO in a reaction cascade, as described earlier. The product, H_2O_2, decomposes at high voltages to release electrons as described by the following equation:

$$H_2O_2 \rightarrow 2H^+ + 1/2O_2 + 2e^-$$

The flow of electrons, i.e., current, is directly proportional to the concentration of hydrogen peroxide produced by the enzyme reactions, which is in turn proportional to the concentration of the analyte (TG).

4.4.2 Fabrication and Response Measurement of an Amperometric TG Biosensor

To construct an amperometric TG biosensor, modified metal electrodes are loaded with enzymes co-immobilized onto nanocomposites, and serve as the working electrode. This electrode along with Ag/AgCl as standard electrode and Pt wire as auxiliary electrode are connected through potentiostat/galvanostat. The three electrode system is immersed into 3 ml of 0.1 *M* phosphate buffer, pH 7.5. Triolein is added into the reaction buffer and current generated due to the enzymatic reaction is measured under an applied potential. The potential applied to electrode with Enz/ZnONPs-CHIT/PtE CHIT-ZnO nanocomposite was 0.4 V (Narang & Pundir, 2011) and 0.1 V, in the case of Enz/AuPPy/pin5COOH/AuE (Narang et al., 2012).

Table 2 Triglycerides Level of Healthy and Diseased Persons as Measured by TG Biosensor Based on Enzyme/AuPPy/Pin5COOH/Au Modified Electrode

		Serum Triglyceride (mg/dl) (Mean ± S.D.)	
Age Group ($n = 8$)	**Sex**	**Healthy Persons**	**Diseased Persons**
11–20	M	90.0 ± 10.4	230.0 ± 15.2
	F	88.3 ± 11.6	210.0 ± 10.1
21–30	M	129.2 ± 43.6	394.1 ± 39.5
	F	105.2 ± 22.3	390.0 ± 57.1
31–40	M	136.2 ± 51.2	422.0 ± 68.1
	F	110.3 ± 30.2	420.0 ± 57.2
41–50	M	164.2 ± 54.6	572.8 ± 51.3
	F	142.1 ± 38.9	413.0 ± 35.4
51 and above	M	195.0 ± 43.5	591.6 ± 54.5
	F	184.2 ± 26.1	495.6 ± 58.3
Range	M	90.0–195.0	230–591.6
	F	88.3–184.2	210–495.6

Reprinted from Narang et al. (2012), with permission from Elsevier.

4.4.3 Analytic Use of TG Biosensor

The TG biosensor is applied for amperometric determination of TG in the serum of healthy people and compared with those suffering from hypertriglyceridemia, and the values have been found to be in the range of 88–195 mg/dl and 210–590 mg/dl, respectively (Table 2) (Narang et al., 2012).

4.4.4 Evaluation of TG Biosensor

Enz/ZnONPs-CHIT electrode has a detection limit (LOD) as low as 20 mg/dl, with the working range 50–650 mg/dl, while Enz/AuPPy/pin5COOH/AuE has the same LOD but slightly higher working range of 50–700 mg/dl. The % recovery of added triolein in the serum is 94–96% as measured by Enz/ZnONPs-CHIT/PtE, but 91–95% by Enz/AuPPy/pin5COOH/AuE (Table 3) (Narang & Pundir, 2011). The coefficient of variation (CV) within and between batches are <3% by Enz/ZnONPs-CHIT/PtE (Table 4) (Narang & Pundir, 2011), while the same are 4.14% and 5.85%, respectively, in case of

Table 3 Analytical Recovery of Added Triglyceride In Sera Determined by TG Biosensor Based on ZnONPs

Triglyceride Added (mg/dl)	Triglyceride Found (mg/dl)	% Recovery
–	180	–
20	199.2	96.0 ± 0.23
50	227.3	94.6 ± 0.40

Reprinted from Narang and Pundir (2011), with permission from Elsevier.

Table 4 Within and Between Batch Assay Coefficient of Variation (CV) for the Determination of Serum Triglyceride by TG Biosensor Based on ZnONPs/CHIT/PtE

n	Triglycerides (mg/dl)	CV (%)
Within assay (5)		
110.89	109.61 ± 1.15	1.04
109		
107.99		
110.4		
109.8		
Between assay (5)		
114.4		2.75
115.5	117.1 ± 3.23	
120.9		
114.4		
120.3		

Reprinted from Narang and Pundir (2011), with permission from Elsevier.

Enz/AuPPy/pin5COOH/AuE. A good correlation was observed ($r = 0.98$–0.99) between the serum triglycerides values obtained by the standard enzymic colorimetric method and these biosensors.

The performance of the TG biosensor is unaffected by a number of serum substances at their corresponding physiological concentrations (Narang & Pundir, 2011) as shown in Table 5.

Table 5 Interference Study of Various Serum Compounds on TG Biosensor Based on ZnONPs

Interferents	Relative Response (%)
Glucose	100
Fructose	100
Ethanol	100
Ascorbic acid	100
Citric acid	100
Lactic acid	100
Malic acid	97
Tartaric acid	100
Alanine	100
Leucine	100
Urea	98
Uric acid	95
Cholesterol	90
Bilirubin	90
Creatinine	100

Reprinted from Narang and Pundir (2011), with permission from Elsevier.

REFERENCES

Barbosa, O., Ortiz, C., Berenguer-Murcia, Á., Torres, R., Rodrigues, R. C., & Fernandez-Lafuente, R. (2015). Strategies for the one-step immobilization-purification of enzymes as industrial biocatalysts. *Biotechnology Advances*, *33*, 435–456.

Barlett, P. N., Dawnson, D. H., & Farrington, J. (1992). Electrochemically polymerized films of 5- carboxyindole. *Journal of Chemical Society Faraday Transaction*, *88*, 2685–2695.

Duff, M., & Kumar, C. V. (2009). Molecular signatures of protein binding to alpha-ZrP: Isothermal titration calorimetric studies. *Journal of Physical Chemistry*, *113*, 15083–15089.

Fossati, P., & Prencipe, L. (1982). Serum triglyceride determined colorimetrically with an enzyme that produces hydrogen peroxide. *Clinical Chemistry*, *28*, 2077–2080.

Jiang, H. L., Kwon, J. T., Kim, Y. K., Kim, E. M., Arote, R., Jeong, H. J., et al. (2007). Galactosylated poly(ethylene glycol)-chitosan-graft-polyethylenimine as a gene carrier for hepatocyte-targeting. *Gene Therapy*, *14*, 1389–1398.

Kalia, V., & Pundir, C. S. (2002). Co-immobilization of lipase, glycerol kinase, glycerol-3-phosphate oxidase and peroxidase onto alkylamine glass beads through glutaraldehyde coupling. *Indian Journal of Biochemistry & Biophysics*, *39*, 342–346.

Kazenwadel, F., Franzreb, M., & Rapp, B. E. (2015). Synthetic enzyme supercomplexes: Co-immobilization of enzyme cascades. *Analytical Methods*, *7*, 4030–4037.

Kalia, V., & Pundir, C. S. (2004). Evaluation of serum triglyceride determination with lipase, glycerol kinase and glycerol-3- phosphate oxidase and peroxidase co-immobilized onto alkylamine glass beads. *Indian Journal of Biochemistry & Biophysics*, *41*, 326–328.

Kumar, C. V., & Chaudhari, A. (2002). High temperature activity of heme proteins at zirconium phosphate. *Chemical Communications*, *20*, 2382–2383.

Kumar, C. V., & Chaudhari, A. (2000). Protein immobilized at the galleries of alpha-zirconium phosphates: Structure and activity studies. *Journal of the American Chemical Society*, *122*, 830–837.

Lata, S., Batra, B., Singala, N., & Pundir, C. S. (2013). Construction of amperometric L-amino acids biosensor based on L-amino acid oxidase immobilized onto ZnONPs/c-MWCNT/PANI/AuE. *Sensors and Actuators B: Chemical*, *188*, 1080–1088.

Liao, J. D., Lin, S. P., & Wu, Y. T. (2005). Dual properties of the deacetylated sites in chitosan for molecular immobilization and biofunctional effects. *Biomacromolecules*, *6*, 392–399.

Miao, Y., Wu, X., Chen, J., Liu, J., & Qiu, J. (2008). Preparation of Au/polypyrrole composite nanoparticles and study of their electro-catalytical reduction to oxygen with (without) lacasse. *Gold Bulletin*, *41*, 336–340.

Minakshi, & Pundir, C. S. (2008a). Co-immobilization of lipase, glycerol kinase, glycerol-3-phosphate oxidase and peroxidase on to aryl amine glass beads affixed on plastic strip for determination of triglycerides in serum. *Indian Journal of Biochemistry & Biophysics*, *42*, 111–115.

Minakshi, & Pundir, C. S. (2008b). Construction of an amperometric enzymic sensor for triglyceride determination. *Sensors Actuators B: Chemical*, *133*, 251–255.

Mudhivarthi, V. K., Bhambhani, A., & Kumar, C. V. (2007). Novel enzyme/DNA/inorganic nanomaterials: A new generation of biocatalysts. *Dalton Transactions*, *21*, 5483–5497.

Narang, J., & Pundir, C. S. (2011). Construction of triglyceride biosensor based on chitosan-ZnO nanocomposite film. *International Journal of Biological Macromolecules*, *49*, 701–705.

Narang, J., Bhambi, M., Minakshi, & Pundir, C. S. (2010). Determination of serum triglyceride by enzyme electrode using covalently immobilized enzyme on egg shell membrane. *International Journal of Biological Macromolecules*, *47*, 691–695.

Narang, J., Chauhan, N., Rani, P., & Pundir, C. S. (2012). Construction of an amperometric biosensor based on AuPPy nanocomposite and poly (indole-5-carboxylic acid) modified Au electrode. *Bioprocess and Biosystems Engineering*, *36*, 425–432.

Nelson, D. M., Cox, M. M., & Lehninger. (2000). *Principles of biochemistry* (4th ed.). New York: Worth publishing. Chapter 6.

Chowdhury, R., Stromer, B. S., Pokharel, B., & Kumar, C. V. (2012). Control of enzyme-solid interactions by chemical modification. *Langmuir*, *28*, 11881–11889.

Novak, M. J., Pattammattel, A., Koshmerl, B., Puglia, M., Williams, C., & Kumar, C. V. (2016). 'Stable-on-the-Table' enzymes: Engineering enzyme-graphene oxide interface for unprecedented stability of the biocatalysts. *ACS Catalysis*, *6*, 339–347.

Pundir, C. S., Singh, S., Bharvi, & Narang, J. (2010). Construction of an amperometric triglyceride biosensor using PVA membrane bound enzymes. *Clinical Biochemistry*, *43*, 467–472.

Singh, S. P., Arya, S. K., Pandey, M. K., Malhotra, B. D., Saha, S., Sreenivas, K., et al. (2007). Cholesterol biosensor based on rf sputtered zinc oxide nanoporous thin film. *Applied Physics Letters*, *91*, 233106.

Vu, Q. T., Pavlik, M., Hebestreit, N., Pfleger, J., Rammelt, U., & Plieth, W. (2005). Electrophoresis deposition of nanocomposites formed from polythiophene abd metal oxides. *Electrochimica Acta*, *51*, 1117–1124.

Wang, J. X., Sun, X. W., Wei, A., Lei, Y., Cai, X. P., Li, C. M., et al. (2006). Zinc oxide nanocomb biosensor for glucose detection. *Applied Physics Letters*, *88*, 233106.

Wei, A., Sun, X. W., Wang, J. X., Lei, Y., Cai, X. P., Li, C. M., et al. (2006). Enzymatic glucose biosensor based on ZnO nanorod array grown by hydrothermal decomposition. *Applied Physics Letters*, *89*, 123902.

Winartasaputra, H., Kutan, S. S., & Cuilbault, G. C. (1982). Amperometric determination of triglyceride in serum. *Analytica Chimica Acta*, *54*, 1987–1990.